haematologica
Journal of the Ferrata Storti Foundation

Genetic alterations of SENP6 in multiple myeloma disrupt genome and proteome stability, sensitizing to proteasome inhibition

by Frederik Herzberg, Michael Korenkov, Konstandina Isaakidis, Chuanbing Zang, Matthias Wirth, Stefan Müller, Ulrich Keller and Uta M. Demel

Received: September 4, 2025.
Accepted: November 24, 2025.

Citation: Frederik Herzberg, Michael Korenkov, Konstandina Isaakidis, Chuanbing Zang, Matthias Wirth, Stefan Müller, Ulrich Keller and Uta M. Demel. Genetic alterations of SENP6 in multiple myeloma disrupt genome and proteome stability, sensitizing to proteasome inhibition.
Haematologica. 2025 Dec 4. doi: 10.3324/haematol.2025.288863 [Epub ahead of print]

LETTER TO THE EDITOR

Genetic alterations of SENP6 in multiple myeloma disrupt genome and proteome stability, sensitizing to proteasome inhibition

Frederik Herzberg[1,2*], Michael Korenkov[1,2*], Konstandina Isaakidis[1,2], Chuanbing Zang[1,2], Matthias Wirth[1,2,3,4], Stefan Müller[4,5], Ulrich Keller[1,2,4,6,7], Uta M. Demel[1,2,8]

[1]Department of Hematology, Oncology and Cancer Immunology, Campus Benjamin Franklin, Charité - Universitätsmedizin Berlin, corporate member of Freie Universität Berlin and Humboldt-Universität zu Berlin, 12203 Berlin, Germany

[2]Max-Delbrück-Center for Molecular Medicine, 13125 Berlin, Germany

[3]Department of General, Visceral and Pediatric Surgery, University Medical Center Göttingen, 37075 Göttingen, Germany

[4]German Consortium for Translational Cancer Research (DKTK), partner site Berlin, German Cancer Research Center (DKFZ), 69120 Heidelberg, Germany

[5]Institute of Biochemistry II, Goethe University Frankfurt, Medical School, 60590 Frankfurt, Germany

[6]National Center for Tumor Diseases (NCT), partner site Berlin, German Cancer Research Center (DKFZ), 69120 Heidelberg, Germany

[7]Cluster of Excellence ImmunoPreCept, Charité - Universitätsmedizin Berlin, Berlin, Germany

[8]Clinician Scientist Program, Berlin Institute of Health (BIH), Berlin, Germany

* shared first authors

Corresponding Author: Uta M. Demel, Department of Hematology, Oncology and Cancer Immunology, Campus Benjamin Franklin, Charité - Universitätsmedizin Berlin, Berlin, Germany, e-mail: uta.demel@charite.de

Running title: SENP6 loss sensitizes to proteasome inhibition

Keywords

SENP6 | SUMO | DNA DAMAGE RESPONSE | UNFOLDED PROTEIN RESPONSE | PROTEASOME INHIBITION

FUNDING

This work was supported by Wilhelm Sander Stiftung grant 2024.109.1 to U.M.D., 2017.048.2 to U.K.; Deutsche Forschungsgemeinschaft (DFG) grant KE222/11-1 project number 508460329 to U.K., KE222/10-1 project number 494535244 to U.K. and S.M., WI 6148/1-1 project number 529255113 to M.W.; Deutsche Krebshilfe grants 70111944, 70114724 and 70116097 to U.K., 70114724 to U.K. and S.M., 70115444 to M.W.; Else Kröner-Fresenius-Stiftung grant 2024_KEA.07 to U.M.D.; Hector Stiftung grant M2506 to U.K., M2408 to M.W., and Stiftung Charité to U.K. U.M.D. is participant in the BIH-Charité Clinician Scientist program funded by the Charité-Universitätsmedizin Berlin und BIH.

ACKNOWLEDGMENTS

We gratefully acknowledge Marlon Schielin for his excellent technical assistance and support with all experiments.

AUTHOR CONTRIBUTIONS

Conception and design of the study by F.H., M.K., U.K. and U.M.D. Acquisition of data and/or analysis and interpretation of data by F.H., M.K., K.I., C.Z., M.W., S.M., U.K. and U.M.D. Drafting of the manuscript by F.H., M.K., U.K. and U.M.D. All authors revised the manuscript for important intellectual content and approved the final version submitted for publication.

COMPETING INTERESTS

All other authors report no conflicts of interest related to this manuscript.

DATA SHARING

The RNA Seq data generated in this study have been stored on the GEO server with the project accession number GSE303255. Further data reported in this paper will be shared by the lead contact upon request.

MAIN TEXT

Targeting of the ubiquitin-proteasome system (UPS) remains a mainstay in the treatment of multiple myeloma (MM), the second most common hematological malignancy, driven by monoclonal plasma cell expansion. Despite major therapeutic advances over the past decades through proteasome inhibitors (PI), immunomodulatory agents (IMiDs), monoclonal antibodies and more recently chimeric antigen receptor (CAR) T-cell therapies and bispecific T-cell engagers, MM remains incurable and nearly all patients relapse. Molecular profiling has identified recurrent genetic alterations with varying clinical outcome, underscoring the disease's heterogeneity [1]. This genetic complexity emphasizes the need for personalized treatment strategies to overcome resistance and improve outcomes, particularly for patients with adverse prognosis. Protein homeostasis in MM critically depends on the UPS [2] and is further regulated by SUMOylation, a closely related post-translational protein modification, which orchestrates key cellular processes, such as cell cycle regulation, DNA repair, transcription and chromatin remodeling [3, 4] by covalently attaching small ubiquitin-like modifiers (SUMO1, SUMO2, SUMO3) to target proteins. Like ubiquitylation, SUMOylation is controlled by a multi-step enzymatic cascade involving activating (SAE1/UBA2) enzymes, conjugating (UBC9) enzymes and ligases, and is fully reversible through SUMO-specific proteases (SENPs) [5]. In cancer this balance is often disrupted and hyperactivation of the SUMO pathway is implicated in disease progression and associated with poor prognosis [6].
In this study we investigated the functional imbalance of dysregulated SUMOylation in MM by analyzing the large CoMMpass dataset for molecular alterations associated with SUMO pathway regulation. Deficiency of key SUMO proteases SENP6 and SENP7 emerged as a critical driver of aberrant SUMOylation dynamics, with recurrent loss of SENP6 being directly linked to adverse prognosis. SENP6 reconstitution markedly reduced cellular growth kinetics in SENP6-deficient MM, indicating a functional role for SENP6 as a tumor suppressor. Mechanistically, SENP6 loss resulted in the accumulation of DNA damage and misfolded proteins, thereby activating the unfolded protein response (UPR), increasing reliance on proteasomal degradation, and driving synthetic lethality to therapeutic PI. Together, we established SENP6 as a functional biomarker and uncovered a mechanistic basis for enhanced PI efficacy in the prognostically unfavorable subgroup of SENP6-deficient MM patients.

Aberrant activation of the SUMOylation pathway is a perceived hallmark of cancer [6]. Reflecting its role in tumor biology of MM, transcriptomic profiling of MM patients revealed an upregulation of the SUMOylation machinery compared to plasma cells from healthy donors (Fig. 1A) [7]. Analysis of the CoMMpass study, one of the largest and most comprehensive human MM datasets, showed a marked upregulation of the SUMO pathway in

relapsed/refractory (R/R) MM compared to newly diagnosed cases (NDMM) (Fig. 1B) [1]. Increased SUMOylation further correlated with advanced International Staging System (ISS) stage (Fig. 1C) and was linked to adverse clinical outcome (Fig. 1D), collectively underscoring a prominent role for enhanced SUMOylation dynamics in MM biology and disease progression. As SENP activity is known to be a direct regulator of SUMOylation, we analyzed the interplay between the SUMO pathway and SUMO chain editing protease activity using a multivariable Cox model in the CoMMPass dataset. Notably, among SENP family members, only SENP6 and SENP7 can process poly-SUMO chains, and deficient poly-SUMO chain editing emerged as a key regulator driving adverse SUMOylation dynamics in MM (Fig. 1E). Analysis of the CoMMpass dataset revealed recurrent arm level deletions of chromosome 6q, encompassing the *SENP6* locus, in ~15% of patients (Fig. 1F), whereas *SENP7* was not affected by copy number loss (Fig. S1A, S1B). This was validated in an independent MM cohort, with 6q/*SENP6* deletions detected in 20% of cases (Fig. S1C) [8]; and no evidence of 3q/*SENP7* loss (Fig. S1D). 6q/*SENP6* loss correlated with reduced *SENP6* mRNA expression (Fig. 1G, S1E) and clinically, low *SENP6* levels were strongly associated with adverse prognosis in two independent datasets (Fig. 1H, S1F) [9]. Compared with myeloma precursor cells, *SENP6* expression was decreased at the time of disease onset (Fig. S1G) [10]. It further declined with advanced ISS stage (Fig. 1I) and was significantly lower in R/R MM patients compared to NDMM cases (Fig. 1J). Moreover, longitudinal analysis of paired BM samples confirmed a progressive decline in *SENP6* expression from first diagnosis to relapse (Fig. 1K). Notably, patient treatment characteristics and high-risk genetic features were largely balanced across patient subgroups of differential *SENP6* expression (Fig. S1H, S1I). Together, we demonstrate that enhanced SUMOylation in MM is linked to recurrent *SENP6* loss, which is associated with disease progression and poor clinical outcome.

To establish mechanistic models, we analyzed the Cancer Cell Line Encyclopedia (CCLE) and identified 11 MM cell lines with genetic *SENP6* loss and 17 with intact *SENP6* locus (Fig. 2A). Ectopic reconstitution of SENP6 in SENP6-deficient AMO-1 and L-363 cells significantly impaired cellular growth (Fig. 2B, 2C), indicating a functional role for SENP6 as a tumor suppressor in MM. Given the inverse correlation between SENP6 expression and SUMOylation in MM patients, we next assessed its functional impact on cellular SUMO homeostasis. SENP6 reconstitution in AMO-1 cells markedly reduced SUMO2/3 and SUMO1 conjugates (Fig. 2D), whereas CRISPR/Cas9-mediated SENP6 depletion ($SENP6^{KD}$) in three cell lines with intact SENP6 locus (MM.1S, NCI-H929, OPM-2) resulted in notable accumulation of SUMO2/3- and SUMO1-conjugated proteins (Fig. S2A, S2B). This effect was more pronounced for SUMO2/3 conjugates compared to SUMO1, consistent with SENP6's preferential affinity for SUMO2/3 conjugates. Further, SENP6 loss resulted in

accumulation of high molecular weight SUMO2/3 conjugates, indicative of impaired poly-SUMO chain editing [5]. Consistently, gene set enrichment analysis (GSEA) of patient samples revealed a significant enrichment of the SUMO conjugation pathway in SENP6-deficient MM (Fig. S2C). Together, these data identify SENP6 as a tumor suppressor and key regulator of SUMO homeostasis in MM.

To systematically investigate the molecular consequences of SENP6 loss in MM, we performed transcriptome profiling of SENP6-depleted MM cells. GSEA revealed enrichment of oncogenic signatures, including “DNA repair” and “unfolded protein response”, indicating increased DNA damage and ER stress upon SENP6 deficiency (Fig. 2E, 2F, S2D, S2E). In line with SENP6’s role in chromatin organization and DNA damage response (DDR) [11, 12, 13], SENP6 depletion impaired DDR signaling, as shown by reduced CHK1 phosphorylation upon DNA-damaging doxorubicin treatment (Fig. 2G). Moreover, a marked increase in γH2AX phosphorylation was detected, indicating a pronounced accumulation of DNA double-strand breaks (Fig. S2F). Consistently, analysis of the CoMMpass dataset reinforced this link, revealing a “DNA damage” signature in SENP6-deficient MM patients (Fig. 2H). Moreover, SENP6-deficient MM cell lines displayed significantly more co-occurring copy number alterations than SENP6-proficient cell lines (Fig. S2G, S2H), further supporting its role as a critical guardian of genome stability in MM. Plasma cells depend on an efficient proteostasis network in the endoplasmic reticulum (ER) to sustain immunoglobulin synthesis, folding, and secretion, rendering them particularly sensitive to ER stress [14]. Defective DNA repair and increased genomic instability promote accumulation of misfolded and unfolded proteins in the ER [15], thereby triggering the UPR as a compensatory response to restore protein homeostasis [16]. In line with increased genotoxic stress, SENP6-deficient MM cells showed robust UPR activation compared to controls (Fig. 2E, 2F, S2E). Immunoblot analysis confirmed elevated UPR signaling, including increased IRE1α expression, enhanced XBP1 splicing, and PERK phosphorylation (Fig. 2I, S2I). To assess the clinical relevance, ssGSEA of the CoMMpass dataset revealed an enrichment of the UPR signature in SENP6-deficient MM patients (Fig. 2J). We here identify SENP6 as a central regulator of ER homeostasis and stress adaptation in MM, highlighting its critical role in maintaining proteostasis through modulation of the UPR. Together, our data position SENP6 as a dual guardian of genome integrity and protein homeostasis in MM by coordinating DDR signaling and ER integrity.

To comprehensively explore therapeutic vulnerabilities to standard-of-care treatments in the clinically unfavorable subgroup of SENP6-deficient MM, we performed a high-throughput image-based drug screen (pharmacoscopy) using the Operetta® CLS microplate imager platform (Fig. 3A). Pharmacoscopy enables highly precise quantification of diverse cellular parameters and markers with unprecedented accuracy due to the large number of events monitored [17]. In detail, control and SENP6-deficient cells were exposed to increasing

concentrations of standard MM drugs for 72h, followed by automated imaging and analysis. Leveraging the open-access drug screening analysis pipeline Breeze2.0 [18], SENP6-deficient cells showed a marked increase in sensitivity to proteasome inhibitors (bortezomib, carfilzomib) (Fig. 3B, 3C). Mechanistically, SENP6 loss impairs DDR and activates the UPR. Misfolded proteins are primarily cleared via ER-associated degradation, which involves retrograde translocation to the cytosol followed by 26S proteasome-mediated degradation [19]. Consequently, SENP6-deficient MM cells became increasingly dependent on proteasomal function to maintain ER integrity, making them particularly vulnerable to PI. On top, SENP6-depleted MM cells displayed enhanced sensitivity to cyclophosphamide and etoposide, both of which induce DNA damage and disproportionately impact cells with impaired cell-cycle checkpoint activation as observed for SENP6 deficiency. In contrast, SENP6-deficient MM cells showed only marginal responses to dexamethasone and no change to melphalan or IMiDs (Fig. 3B, 3C). These findings were validated across an informative MM cell line panel. Accordingly, SENP6 depletion increased sensitivity to both bortezomib and carfilzomib treatment (Fig. 3D-3G, S3A-B), consistent with enhanced apoptosis rates (Fig. S3C-D). In support of our findings, ectopic SENP6 reconstitution in AMO-1 and L-363 cells conferred resistance to PI treatment (Fig. S3E-H). In summary, these data provide a mechanistic rationale for enhanced efficacy of proteasome inhibition in the subgroup of SENP6-depleted MM.

In this study, we uncovered a critical role for enhanced SUMOylation dynamics in MM biology. By integrating patient data with mechanistic studies, we identified recurrent deletions of SENP6 as a molecular feature of a clinically unfavorable MM subgroup. Functionally, loss of SENP6 drives excessive poly-SUMOylation, impairing DNA repair, genomic stability, and protein homeostasis. These vulnerabilities activate the UPR and increase reliance on proteasomal degradation, creating synthetic lethality to therapeutic PI. Despite this initial PI vulnerability, SENP6-deficient MM patients exhibit poorer outcomes, indicating that additional mechanisms may limit therapeutic efficacy over time. Mechanistically, we demonstrate a critical role for SENP6 in preserving genomic integrity by guarding DNA repair. Maintenance of genomic stability is essential for cellular homeostasis, and its loss fosters oncogenic evolution. Accordingly, SENP6 deficiency is associated with increased genomic instability in MM, potentially driving tumor evolution and progression.

All experiments were performed in compliance with national guidelines and the principles of good scientific practice to ensure accuracy, reproducibility, and integrity of the data.

REFERENCES

1. Skerget S, Penaherrera D, Chari A, et al. Comprehensive molecular profiling of multiple myeloma identifies refined copy number and expression subtypes. Nat Genet. 2024;56(9):1878-1889.
2. Lub S, Maes K, Menu E, De Bruyne E, Vanderkerken K, Van Valckenborgh E. Novel strategies to target the ubiquitin proteasome system in multiple myeloma. Oncotarget. 2016;7(6):6521-6537.
3. Flotho A, Melchior F. Sumoylation: a regulatory protein modification in health and disease. Annu Rev Biochem. 2013;82:357-385.
4. Vertegaal ACO. Signalling mechanisms and cellular functions of SUMO. Nat Rev Mol Cell Biol. 2022;23(11):715-731.
5. Kunz K, Piller T, Muller S. SUMO-specific proteases and isopeptidases of the SENP family at a glance. J Cell Sci. 2018;131(6):jcs211904.
6. Seeler JS, Dejean A. SUMO and the robustness of cancer. Nat Rev Cancer. 2017;17(3):184-197.
7. Chauhan D, Tian Z, Nicholson B, et al. A small molecule inhibitor of ubiquitin-specific protease-7 induces apoptosis in multiple myeloma cells and overcomes bortezomib resistance. Cancer Cell. 2012;22(3):345-358.
8. Chapman MA, Lawrence MS, Keats JJ, et al. Initial genome sequencing and analysis of multiple myeloma. Nature. 2011;471(7339):467-472.
9. Hanamura I, Stewart JP, Huang Y, et al. Frequent gain of chromosome band 1q21 in plasma-cell dyscrasias detected by fluorescence in situ hybridization: incidence increases from MGUS to relapsed myeloma and is related to prognosis and disease progression following tandem stem-cell transplantation. Blood. 2006;108(5):1724-1732.
10. Boiarsky R, Haradhvala NJ, Alberge JB, et al. Single cell characterization of myeloma and its precursor conditions reveals transcriptional signatures of early tumorigenesis. Nat Commun. 2022;13(1):7040.
11. Wagner K, Kunz K, Piller T, et al. The SUMO Isopeptidase SENP6 Functions as a Rheostat of Chromatin Residency in Genome Maintenance and Chromosome Dynamics. Cell Rep. 2019;29(2):480-494.e485.
12. Schick M, Zhang L, Maurer S, et al. Genetic alterations of the SUMO isopeptidase SENP6 drive lymphomagenesis and genetic instability in diffuse large B-cell lymphoma. Nat Commun. 2022;13(1):281.
13. Liebelt F, Jansen NS, Kumar S, et al. The poly-SUMO2/3 protease SENP6 enables assembly of the constitutive centromere-associated network by group deSUMOylation. Nat Commun. 2019;10(1):3987.
14. Vincenz L, Jager R, O'Dwyer M, Samali A. Endoplasmic reticulum stress and the unfolded protein response: targeting the Achilles heel of multiple myeloma. Mol Cancer Ther. 2013;12(6):831-843.
15. Gonzalez-Quiroz M, Blondel A, Sagredo A, Hetz C, Chevet E, Pedeux R. When Endoplasmic Reticulum Proteostasis Meets the DNA Damage Response. Trends Cell Biol. 2020;30(11):881-891.
16. Hetz C, Zhang K, Kaufman RJ. Mechanisms, regulation and functions of the unfolded protein response. Nat Rev Mol Cell Biol. 2020;21(8):421-438.
17. Kropivsek K, Kachel P, Goetze S, et al. Ex vivo drug response heterogeneity reveals personalized therapeutic strategies for patients with multiple myeloma. Nat Cancer. 2023;4(5):734-753.
18. Potdar S, Ianevski F, Ianevski A, et al. Breeze 2.0: an interactive web-tool for visual analysis and comparison of drug response data. Nucleic Acids Res. 2023;51(W1):W57-W61.
19. Obeng EA, Carlson LM, Gutman DM, Harrington WJ Jr., Lee KP, Boise LH. Proteasome inhibitors induce a terminal unfolded protein response in multiple myeloma cells. Blood. 2006;107(12):4907-4916.

FIGURE LEGENDS

Figure 1. Enhanced SUMOylation dynamics driven by SENP6 loss are linked to disease progression and adverse prognosis in MM. (A–C) ssGSEA enrichment scores for the Reactome gene set "SUMOylation" in **(A)** healthy donors (n = 6) vs. newly diagnosed MM (NDMM, n = 170) (Chauhan et al.), **(B)** NDMM (n = 764) vs. relapsed/refractory MM (RRMM, n = 80) and **(C)** across ISS stages I–III in the CoMMpass cohort. **(D)** Kaplan–Meier overall survival curve of MM patients in the CoMMpass cohort stratified by ssGSEA enrichment scores for the Reactome gene set "SUMOylation". **(E)** Forest plot of interaction cox analysis displaying HR of depicted z-standardized reactome pathways in the CoMMpass cohort. Pathway interaction surface visualizing the joint effect of high SUMO pathway and low SUMO chain editing protease activity on overall survival. **(F– G)** SENP6 copy number alterations **(F)** and corresponding expression TPM **(G)** in CoMMpass cohort. Wildtype n= 686; 6q del n= 128; 6q gain = 65. **(H)** Kaplan–Meier overall survival curve of MM patients in the CoMMpass cohort stratified by SENP6 expression. **(I–K)** SENP6 expression of MM patients in the CoMMpass cohort across ISS stages **(I)**, in NDMM vs. RRMM **(J)**, and in paired patient samples at diagnosis and relapse (n = 47) **(K)**. Box and whisker plots indicate minimum to maximum distribution and the mean. P values calculated by Mann–Whitney U (**A, B, J)**, Kruskal–Wallis ANOVA with Tukey's post hoc test **(C, I)**, Wilcoxon matched-pairs test **(K)**, or log-rank test **(D, H)**.

Figure 2. SENP6 safeguards SUMO homeostasis and protects genome stability and proteome integrity in multiple myeloma. (A) Expression analysis of SENP6 mRNA in MM cell lines (n=28). **(B)** Immunoblot analysis of SENP6 protein expression upon SENP6 reconstitution versus empty vector (EV) transduction in AMO-1 and L-363 cells. SENP6 protein expression was normalized to β-actin for quantification. **(C)** Analysis of cell proliferation upon SENP6 reconstitution versus EV transduction in AMO-1 and L-363 cells. **(D)** Immunoblot analysis of global SUMO2/3 and SUMO1 modification in AMO-1 cells upon SENP6 reconstitution versus EV transduction. **(E, F)** GSEA of NCI-H929 control vs. SENP6KD **(E)**, highlighting enrichment of DNA damage response (DDR) and unfolded protein response (UPR)-related pathways **(F)**. **(G)** Immunoblot analysis of DDR-related proteins in MM.1S control and SENP6KD following doxorubicin (DRB, 0.5 μM) treatment at indicated time points. **(H)** ssGSEA enrichment scores for the Hallmark "DNA damage" gene set in SENP6 low (n = 211) vs. SENP6 high (n = 633) samples from the CoMMpass cohort. **(I)** Immunoblot analysis of UPR markers in MM.1S control and SENP6KD cells. **(J)** ssGSEA enrichment scores for the Hallmark "UPR" gene set in SENP6 low (n = 211) vs. SENP6 high (n = 633) samples from the CoMMpass cohort. Data represent the mean ± SD in **(B)** and **(C)**. Box and whisker plots indicate minimum to maximum distribution and the mean in **(H)** and **(J)**. P values were calculated by unpaired t-test **(B, C)**. P values calculated by Kolmogorov–Smirnov- **(F)** and Mann–Whitney U-Test **(H, J)**.

Figure 3. High-throughput image-based drug screening discovers synthetic lethality to proteasome inhibition in SENP6-deficient MM. (A) Workflow of the high-content image-based drug testing platform (Operetta) to exploit treatment strategies in SENP6 deficient MM. Cells were stained with DAPI and live/dead stain before imaging. **(B)** Drug sensitivity scores (DSS) of MM.1S control and SENP6KD cells upon treatment with indicated drugs and as outlined in **(A)** were calculated by

BREEZE drug screen analysis pipeline. Heatmap was generated by ClustVis data visualizing tool. **(C)** Representative images of MM.1S control and SENP6KD cells upon bortezomib and carfilzomib treatment with indicated concentrations for 72h. **(D, F)** Dose–response curves for bortezomib and carfilzomib in control and SENP6KD MM.1S **(D)** and NCI-H929 **(F)**. Cells were treated for 72□h and viability was assessed by DAPI-based flow cytometry. **(E, G)** Representative DAPI-Annexin-V dot plots for control and carfilzomib shown in **(E, G)**. Dose–response curves represent mean ± standard deviation **(D, F)**. P values determined by unpaired t-test **(D, F).**

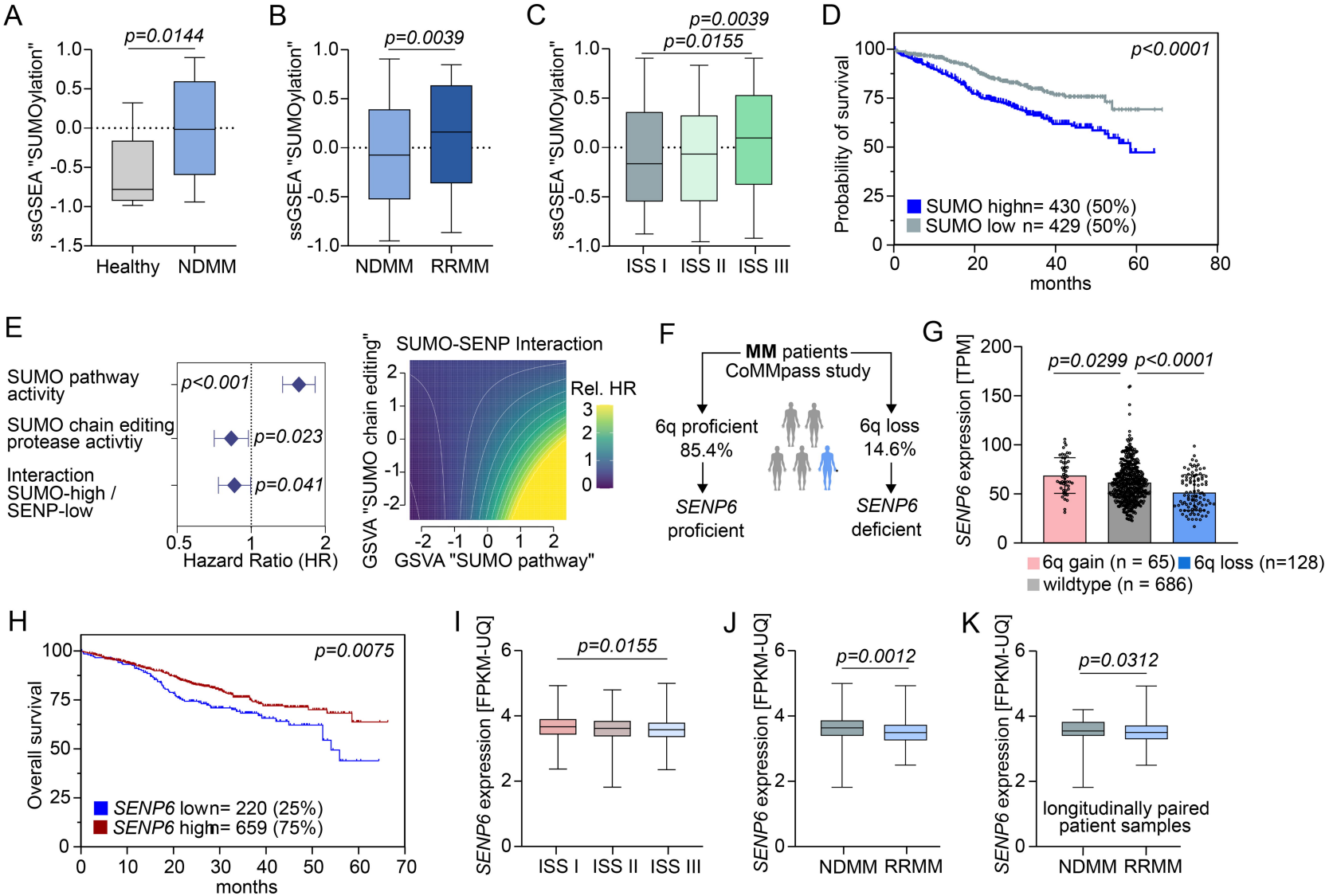
A
p=0.0144
ssGSEA "SUMOylation"
Healthy
NDMM
B
p=0.0039
NDMM
RRMM
C
p=0.0039
p=0.0155
ISS I
ISS II
ISS III
D
p<0.0001
Probability of survival
SUMO highn= 430 (50%)
SUMO low n= 429 (50%)
months
E
SUMO pathway activity
SUMO chain editing protease activtiy
Interaction SUMO-high / SENP-low
p<0.001
p=0.023
p=0.041
Hazard Ratio (HR)
SUMO-SENP Interaction
GSVA "SUMO chain editing"
GSVA "SUMO pathway"
Rel. HR
F
MM patients
CoMMpass study
6q proficient
85.4%
6q loss
14.6%
SENP6
proficient
SENP6
deficient
G
p=0.0299
p<0.0001
SENP6 expression [TPM]
6q gain (n = 65)
6q loss (n=128)
wildtype (n = 686)
H
p=0.0075
Overall survival
SENP6 lown= 220 (25%)
SENP6 highn= 659 (75%)
months
I
p=0.0155
SENP6 expression [FPKM-UQ]
ISS I
ISS II
ISS III
J
p=0.0012
NDMM
RRMM
K
p=0.0312
longitudinally paired patient samples
NDMM
RRMM

Figure 1.

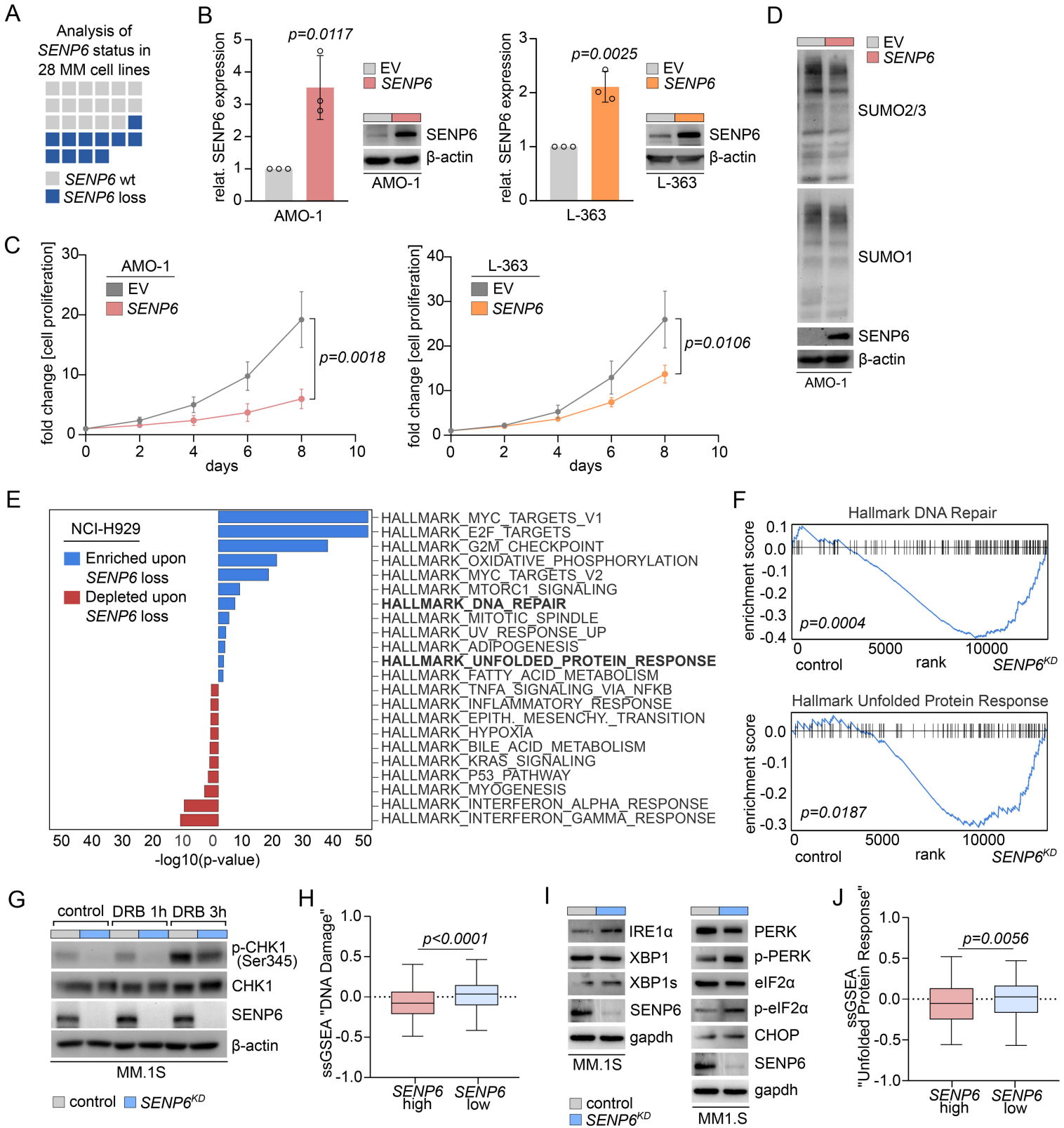
A
Analysis of SENP6 status in 28 MM cell lines
SENP6 wt
SENP6 loss
B
p=0.0117
relat. SENP6 expression
EV
SENP6
SENP6
β-actin
AMO-1
p=0.0025
L-363
C
AMO-1
L-363
fold change [cell proliferation]
days
p=0.0018
p=0.0106
D
SUMO2/3
SUMO1
E
NCI-H929
Enriched upon SENP6 loss
Depleted upon SENP6 loss
HALLMARK_MYC_TARGETS_V1
HALLMARK_E2F_TARGETS
HALLMARK_G2M_CHECKPOINT
HALLMARK_OXIDATIVE_PHOSPHORYLATION
HALLMARK_MYC_TARGETS_V2
HALLMARK_MTORC1_SIGNALING
HALLMARK_DNA_REPAIR
HALLMARK_MITOTIC_SPINDLE
HALLMARK_UV_RESPONSE_UP
HALLMARK_ADIPOGENESIS
HALLMARK_UNFOLDED_PROTEIN_RESPONSE
HALLMARK_FATTY_ACID_METABOLISM
HALLMARK_TNFA_SIGNALING_VIA_NFKB
HALLMARK_INFLAMMATORY_RESPONSE
HALLMARK_EPITH._MESENCHY._TRANSITION
HALLMARK_HYPOXIA
HALLMARK_BILE_ACID_METABOLISM
HALLMARK_KRAS_SIGNALING
HALLMARK_P53_PATHWAY
HALLMARK_MYOGENESIS
HALLMARK_INTERFERON_ALPHA_RESPONSE
HALLMARK_INTERFERON_GAMMA_RESPONSE
-log10(p-value)
F
Hallmark DNA Repair
enrichment score
p=0.0004
control
rank
SENP6KD
Hallmark Unfolded Protein Response
p=0.0187
G
control
DRB 1h
DRB 3h
p-CHK1 (Ser345)
CHK1
SENP6
β-actin
MM.1S
control
SENP6KD
H
ssGSEA "DNA Damage"
p<0.0001
SENP6 high
SENP6 low
I
IRE1α
XBP1
XBP1s
SENP6
gapdh
MM.1S
PERK
p-PERK
eIF2α
p-eIF2α
CHOP
SENP6
gapdh
MM1.S
J
ssGSEA "Unfolded Protein Response"
p=0.0056

Figure 2.

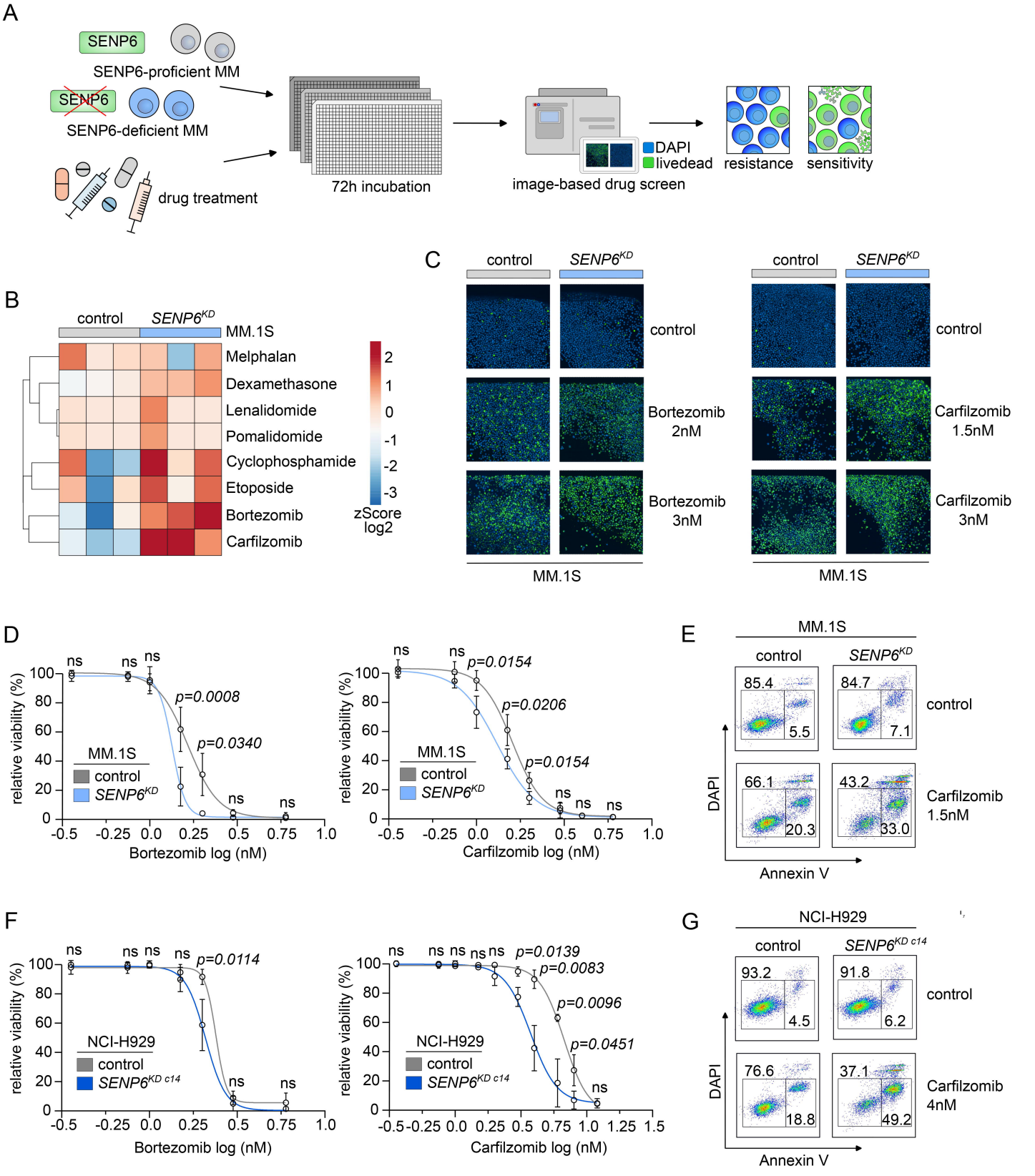
A
SENP6
SENP6-proficient MM
SENP6
SENP6-deficient MM
drug treatment
72h incubation
DAPI
livedead
image-based drug screen
resistance
sensitivity
B
control
SENP6KD
MM.1S
Melphalan
Dexamethasone
Lenalidomide
Pomalidomide
Cyclophosphamide
Etoposide
Bortezomib
Carfilzomib
2
1
0
-1
-2
-3
zScore
log2
C
control
SENP6KD
control
Bortezomib
2nM
Bortezomib
3nM
Carfilzomib
1.5nM
Carfilzomib
3nM
MM.1S
MM.1S
D
relative viability (%)
MM.1S
control
SENP6KD
ns
p=0.0008
p=0.0340
Bortezomib log (nM)
p=0.0154
p=0.0206
p=0.0154
Carfilzomib log (nM)
E
MM.1S
control
SENP6KD
85.4
5.5
84.7
7.1
66.1
20.3
43.2
33.0
control
Carfilzomib
1.5nM
DAPI
Annexin V
F
NCI-H929
control
SENP6KD c14
p=0.0114
Bortezomib log (nM)
p=0.0139
p=0.0083
p=0.0096
p=0.0451
Carfilzomib log (nM)
G
NCI-H929
control
SENP6KD c14
93.2
4.5
91.8
6.2
76.6
18.8
37.1
49.2
control
Carfilzomib
4nM
DAPI
Annexin V

SUPPLEMENTAL FIGURES

Genetic alterations of SENP6 in multiple myeloma disrupt genome and proteome stability sensitizing to proteasome inhibition

Frederik Herzberg[1,2*], Michael Korenkov[1,2*], Konstandina Isaakidis[1,2], Chuanbing Zang[1,2], Matthias Wirth[1,2,3,4], Stefan Müller[4,5], Ulrich Keller[1,2,4,6,7], Uta M. Demel[1,2,8]

[1] Department of Hematology, Oncology and Cancer Immunology, Campus Benjamin Franklin, Charité - Universitätsmedizin Berlin, corporate member of Freie Universität Berlin and Humboldt-Universität zu Berlin, 12203 Berlin, Germany
[2] Max-Delbrück-Center for Molecular Medicine, 13125 Berlin, Germany
[3] Department of General, Visceral and Pediatric Surgery, University Medical Center Göttingen, 37075 Göttingen, Germany
[4] German Consortium for Translational Cancer Research (DKTK), partner site Berlin, German Cancer Research Center (DKFZ), 69120 Heidelberg, Germany
[5] Institute of Biochemistry II, Goethe University Frankfurt, Medical School, 60590 Frankfurt, Germany
[6] National Center for Tumor Diseases (NCT), partner site Berlin, German Cancer Research Center (DKFZ), 69120 Heidelberg, Germany
[7] Cluster of Excellence ImmunoPreCept, Charité - Universitätsmedizin Berlin, Berlin, Germany
[8] Clinician Scientist Program, Berlin Institute of Health (BIH), Berlin, Germany

* shared first authors

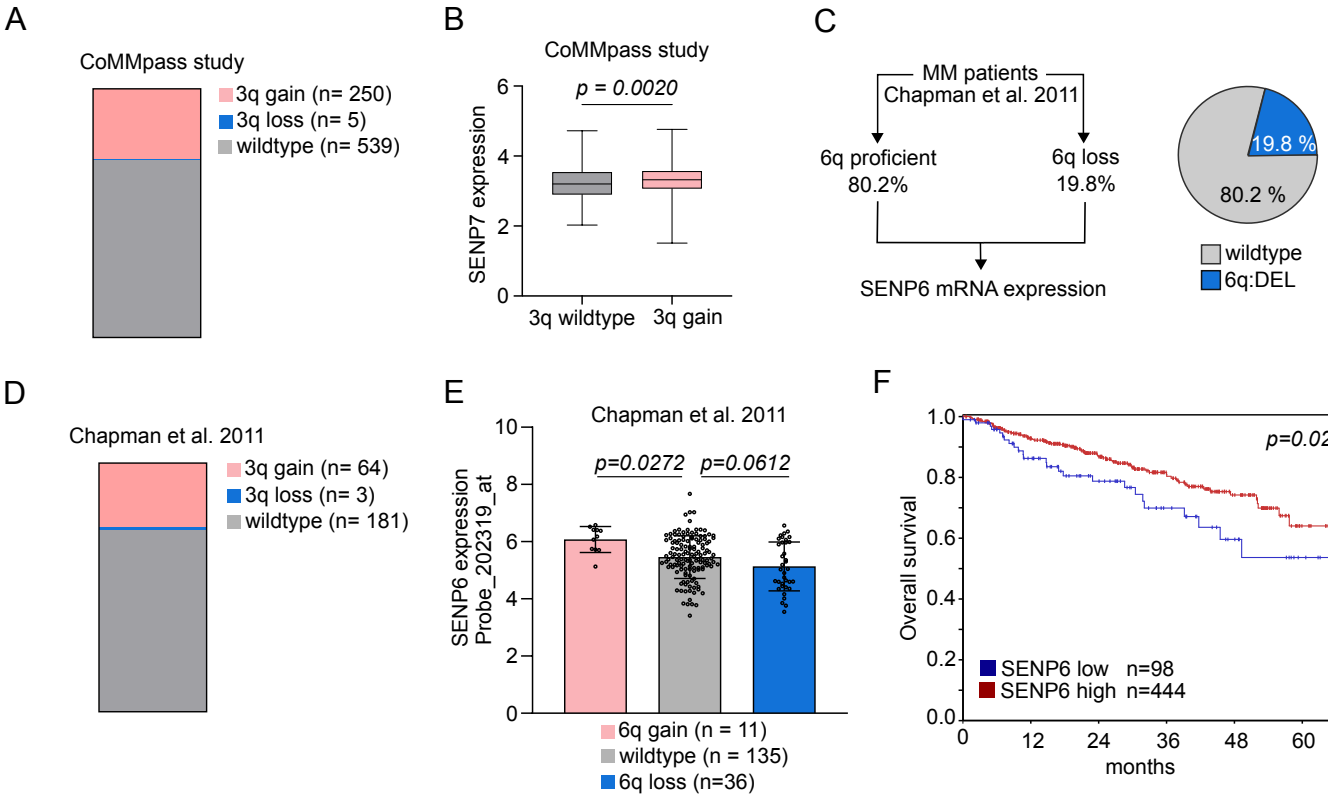

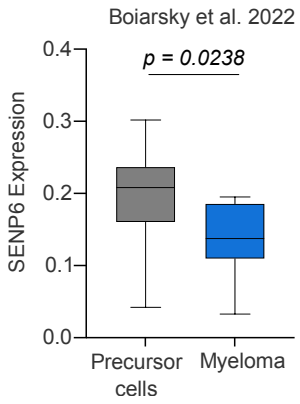

H

Characteristic	Overall	*SENP6* low	*SENP6* high
Chr. 6 gain	80 (10.7%)	1 (0.6%)	79 (13.9%)
Chr. 6 loss	51 (6.8%)	47 (26.7%)	4 (0.7%)
Genetic Characteristics			
High-risk cytogenetics	214 (30.2%)	65 (38.5%)	149 (27.6%)
t(11;14)	147 (20.2%)	14 (8.0%)	133 (24.1%)
Del(17p)	94 (12.6%)	30 (17.0%)	64 (11.2%)
t(14;16)	27 (3.7%)	9 (5.1%)	18 (3.3%)
Treatment Characteristics			
ASCT	441 (51.3%)	113 (52.8%)	328 (50.9%)
Lines of therapy			
n=1	574 (66.8%)	127 (59.3%)	447 (69.3%)
n=2	161 (18.7%)	59 (27.6%)	102 (15.8%)
n=3	70 (8.1%)	21 (9.8%)	49 (7.6%)
n=4	54 (6.3%)	7 (3.3%)	47 (7.3%)

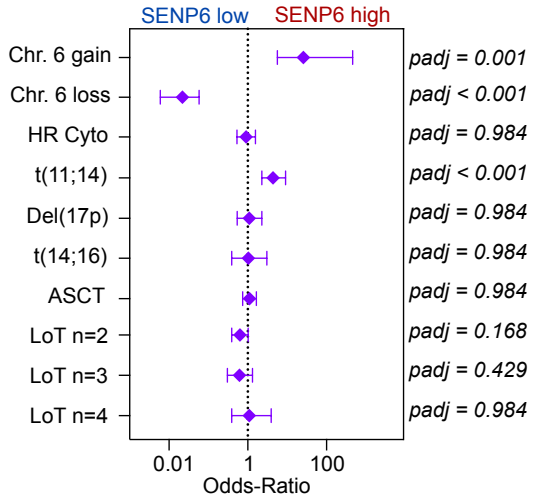

Supplementary Figure S1. (A) Frequency of SENP7 (3q) copy-number alterations in patients with multiple myeloma (MM) from the CoMMpass study. **(B)** SENP7 mRNA expression stratified by copy-number status in the CoMMpass cohort. **(C)** Frequency of SENP6 (6q) copy-number alterations in MM patients from the Chapman dataset. **(D)** Frequency of SENP7 (3q) copy-number alterations in MM patients from the Chapman dataset. **(E)** SENP6 mRNA expression stratified by copy-number status in the Chapman cohort. **(F)** Kaplan-Meier overall survival of patients grouped by SENP6 expression in the Hanamura cohort (GSE2658). **(G)** SENP6 mRNA expression in pseudobulked single plasma cells from precursor (MGUS, SMM) and MM from Bojarsky et al. 2022. **(H)** Patient characteristics table of patients from CoMMpass study. MM patients were grouped by SENP6 mRNA expression levels. **(I)** Forest plot of adjusted odds ratios (95% CI) from a multivariable logistic regression of SENP6 high vs low groups including covariates from **(H)**; LoT: Line of Therapy, HR Cyto: High risk cytogenetics. BH FDR has been applied across coefficients. P-values are reported as adjusted (padj). Bar plot represent mean ± standard deviation in **(B, E)**. P values calculated by Mann Whitney U test **(B, G)**, ANOVA with Tukey's post hoc test **(E)** and log-rank Mantel-Cox test **(F)**.

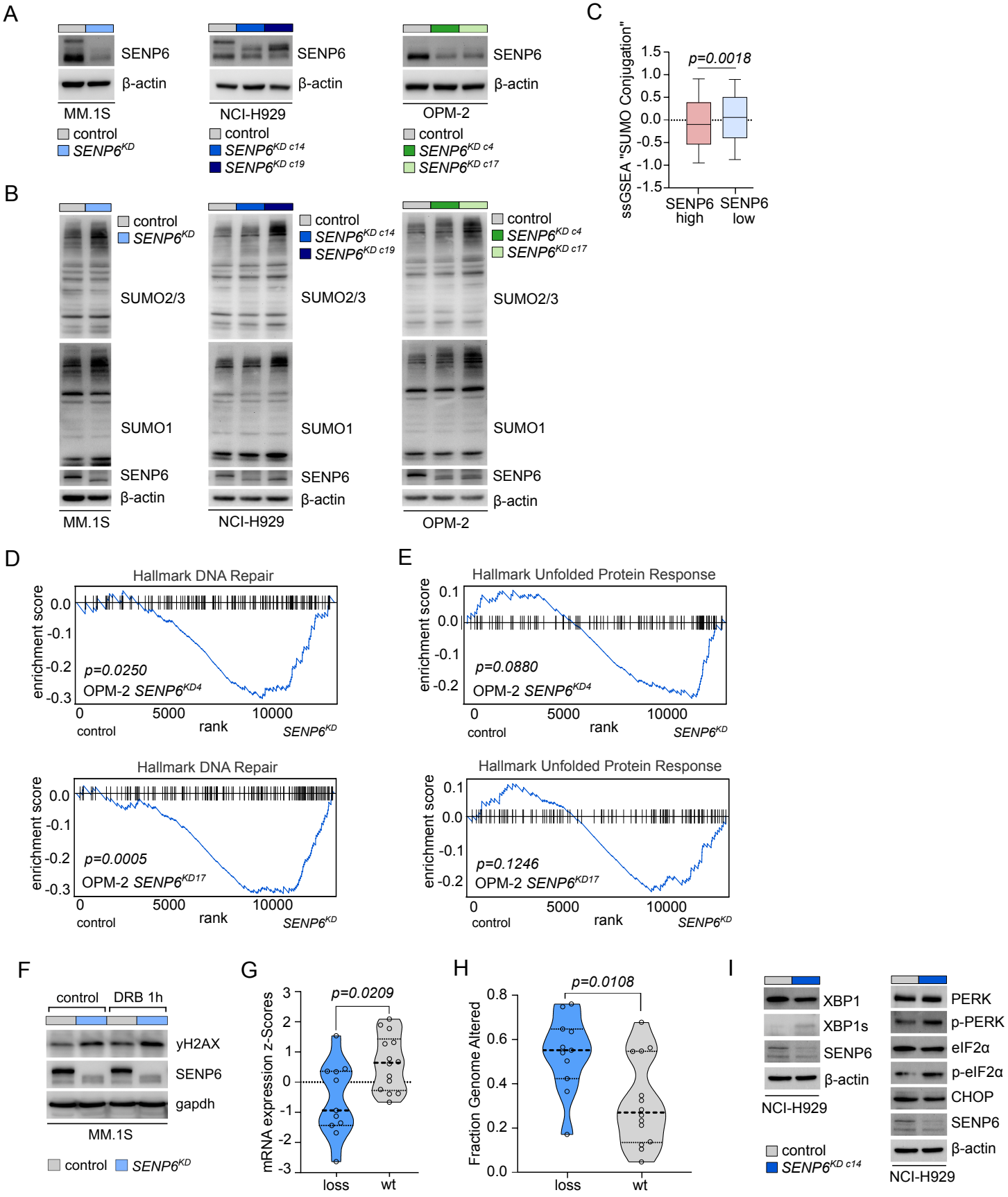

Supplementary Figure S2. (A–B) Immunoblot analysis of global SUMO2/3 and SUMO1 modification in MM.1S, NCI-H929, and OPM-2 cells following CRISPR/Cas9-mediated SENP6 knockdown (KD) **(B)**; **(A)** shows SENP6 protein expression in the indicated cell lines upon SENP6KD. **(C)** ssGSEA analysis of gene set "SUMO Conjugation" of expression data derived from the GDC MMRF CoMMpass dataset. SENP6 was grouped according to mRNA expression levels as follows: SENP6 low = 1st quartile (n= 211), SENP6 high = 2nd to 4th quartile (n= 633). **(D, E)** Gene Set Enrichment Analysis (GSEA) of expression data from transcriptome profiling of OPM-2 control and SENP6KD cells for the gene sets **(D)** "DNA Repair" and **(E)** "Unfolded Protein Response". **(F)** Immunoblot analysis of DDR-related protein γH2AX in MM.1S control and SENP6KD following doxorubicin (DRB, 0.5 μM) treatment at indicated time points. **(G)** Expression analysis of SENP6 mRNA in MM cell lines listed in the cancer cell line encyclopedia (CCLE) (n=28). Groups were classified according to their SENP6 copy number status. **(H)** Analysis of somatic copy number alterations (SCNAs) in MM cell lines (n=28). Groups were classified according to their SENP6 copy number status. **(I)** Immunoblot analysis of indicated UPR markers in NCI-H929 control and SENP6KD cells. Box and whisker plots indicate minimum to maximum distribution and the mean in **(C)**. P values were calculated by Mann-Whitney U test **(C, G, H)** and by Kolmogorov-Smirnov test **(D, E)**.

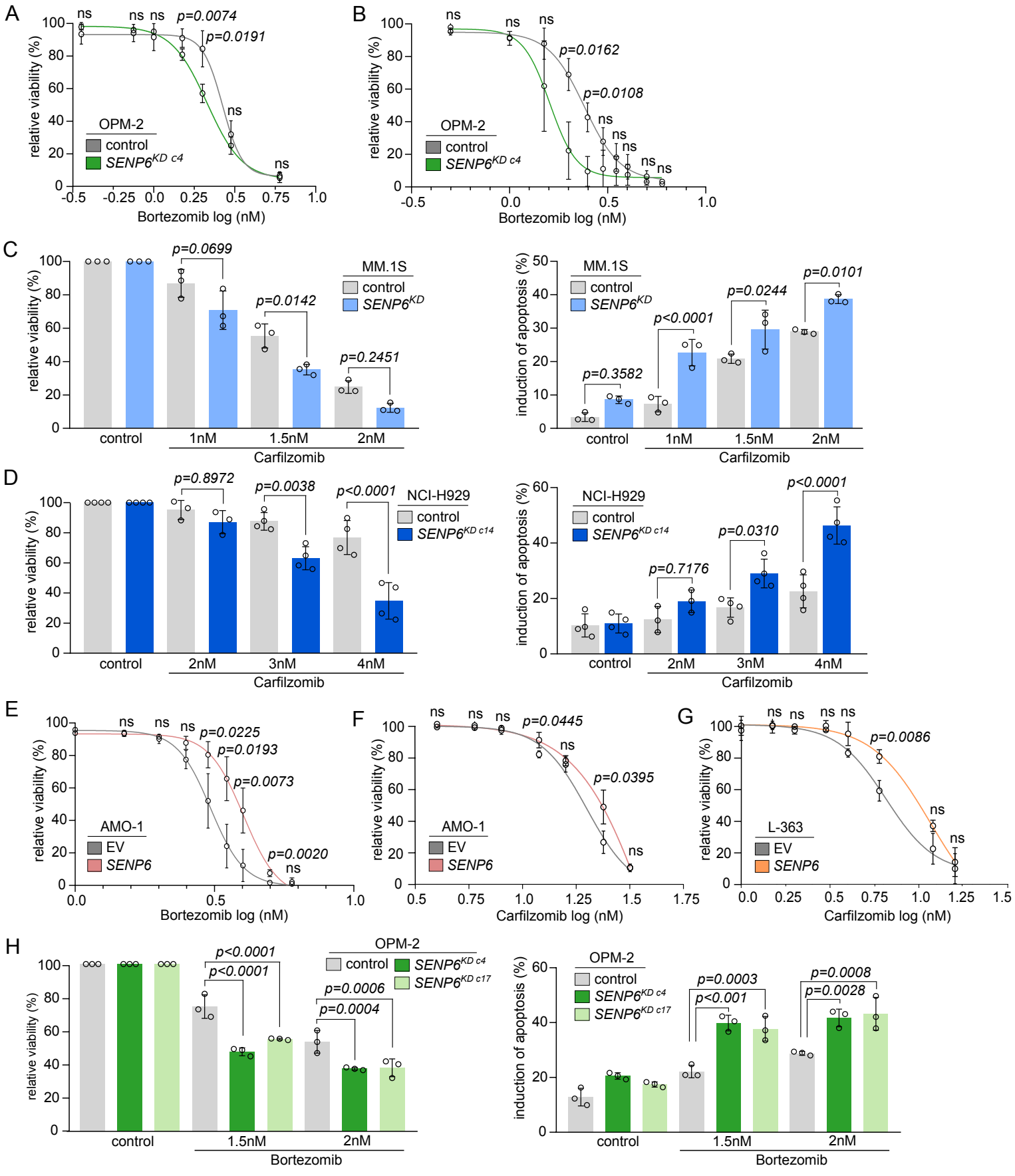

Supplementary Figure S3. (A) Bortezomib dose-response curves of control and SENP6KD OPM-2 cells. Cells were treated for 72h and viability was determined by DAPI flow cytometry measurement. **(B)** Bortezomib dose-response curves of control and SENP6KD OPM-2 cells. Cells were treated for 72h and viability was determined by MTT cell viability assay. **(C, D)** Quantification of viable and apoptotic fractions in control vs. SENP6KD cells after 72 h carfilzomib treatment in MM.1S **(C)** and NCI-H929 **(D). (E)** Bortezomib dose-response curves of upon SENP6 reconstitution versus EV transduction in AMO-1 cells. Cells were treated for 72h and viability was determined by MTT cell viability assay. **(F-G)** Carfilzomib dose-response curves of upon SENP6 reconstitution versus EV transduction in AMO-1 **(F)** and L-363 **(G)** cells. Cells were treated for 72h and viability was determined by DAPI flow cytometry measurement. **(H)** Relative viability and apoptosis in control and SENP6KD OPM-2 cells after bortezomib treatment for 72h. Bar plots and dose–response curves represent mean ± standard deviation **(A-H)**. P values determined by unpaired t-test **(A, B, E-G)** or one-way ANOVA with Tukey's post hoc test **(C, D, H)**.